Mon. Not. R. Astron. Soc. **000**, 1–?? (2013) Printed 6 September 2016 (MN LATEX style file v2.2)

New thresholds for Primordial Black Hole formation during the QCD phase transition

J. L. G. Sobrinho[1,2⋆], P. Augusto[1,2]†, and A. L. Gonçalves[1]‡
[1] *Faculdade de Ciências Exatas e da Engenharia, Universidade da Madeira, Caminho da Penteada, 9000-390 Funchal, Portugal*
[2] *Centro de Astronomia e Astrofísica da Universidade de Lisboa, Tapada da Ajuda, Edifício Leste, 2° piso, 1349-018 Lisboa, Portugal*

arXiv:1609.01205v1 [astro-ph.CO] 5 Sep 2016

Accepted xxxx. Received xxxx; in original form xxxx

ABSTRACT
Primordial Black Holes (PBHs) might have formed in the early Universe as a consequence of the collapse of density fluctuations with an amplitude above a critical value δ_c: the formation threshold. Although for a radiation-dominated Universe δ_c remains constant, if the Universe experiences some dust-like phases (e.g. phase transitions) δ_c might decrease, improving the chances of PBH formation. We studied the evolution of δ_c during the QCD phase transition epoch within three different models: Bag Model (BM), Lattice Fit Model (LFM), and Crossover Model (CM). We found that the reduction on the background value of δ_c can be as high as 77% (BM), which might imply a $\sim 10^{-10}$ probability of PBHs forming at the QCD epoch.

Key words: black hole physics – cosmology: early Universe – cosmology: inflation

1 INTRODUCTION

Primordial Black Holes (PBHs) may have formed in the early Universe as a consequence of the collapse of density fluctuations (e.g. Hawking 1971; Carr & Hawking 1974; Carr 1975; Novikov et al. 1979; Polarski & Dolgov 2001; Khlopov 2010). They might even be directly detectable within our neighboorhood (Sobrinho & Augusto 2014). During inflation, fluctuations of quantum origin are stretched to scales much larger than the cosmological horizon R_H at the time t when they were produced ($R_H(t) = c/H(t)$, with $H(t)$ the Hubble parameter). Once a physical wavelength becomes larger than R_H, it is causally disconnected from physical processes. The inflationary era is followed, respectively, by radiation-dominated and matter-dominated epochs during which these fluctuations can re-enter the cosmological horizon (e.g. Boyanovsky, de Vega, & Schwarz 2006). For a given physical scale k, the horizon crossing time t_k (i.e. the instant when that scale re-enters R_H) is conventionally defined by (e.g. Blais et al. 2003; Bringmann, Kiefer, & Polarski 2002)

$$ck = a(t_k)H(t_k) \tag{1}$$

where $a(t)$ represents the scale factor. The collapse that gives rise to the formation of a PBH is now possible but only if the amplitude of the density fluctuation (δ) is larger than a specific threshold value δ_c. In this case the expansion of the overdense region will, eventually, come to a halt, followed by its collapse. The majority of the PBHs formed at a particular epoch have masses within the order of the horizon mass, M_H, at that epoch (e.g. Carr 2003) given by

$$M_H(t) \sim 10^{15} \left(\frac{t}{10^{-23}\ \mathrm{s}}\right)\ \mathrm{g}. \tag{2}$$

However, in the case of perturbations with δ only slightly larger than the critical value, δ_c, the PBH masses rather obey the scaling law (Niemeyer & Jedamzik 1999)

$$M_{PBH} \propto M_H\,(\delta - \delta_c)^{\gamma} \tag{3}$$

where $\gamma \approx 0.36$ in the case of a radiation-dominated Universe. This power law scaling has been found to hold down to $(\delta - \delta_c) \sim 10^{-10}$ (Musco, Miller, & Polnarev 2009; Musco & Miller 2013).

The probability that a fluctuation crossing the horizon at some instant t_k has of collapsing and forming a PBH can be written as (e.g. Green 2015)

$$\beta(t_k) = \frac{1}{\sqrt{2\pi}\sigma(t_k)} \int_{\delta_c}^{\infty} \exp\left(-\frac{\delta^2}{2\sigma^2(t_k)}\right) d\delta \tag{4}$$

where $\sigma^2(t_k)$ is the mass variance at horizon crossing.

Carr (1975), based on a simplified model of an overdense collapsing region, found $\delta_c = 1/3$ for a radiation-dominated Universe. In more recent years the threshold δ_c has been extensively investigated by numerical simulations in PBH formation, in particular by numerically solving relativistic hydrodynamical equations (see e.g. Musco, Miller, & Rezzolla 2005). Although Niemeyer & Jedamzik (1999) reported the value $\delta_c \simeq 0.7$ in the case of a radiation-

⋆ E-mail: sobrinho@uma.pt (JLGS)
† E-mail: sciman@med.up.pt (PA)
‡ E-mail: angel@uma.pt (ALG)

© 2013 RAS

dominated expanding Universe, this was later revised to $\delta_c \simeq 0.43 - 0.47$ (Musco, Miller, & Rezzolla 2005; Polnarev & Musco 2007; Musco, Miller, & Polnarev 2009; Harada, Yoo, & Kohri 2013; Musco & Miller 2013). Usually δ_c is constant throught the radiation-dominated epoch, the exception occurring during cosmological phase transitions, when the value of δ_c decreases (as a consequence of the decrease of the sound speed). This is relevant, since a lower value of δ_c favours PBH production (e.g. Carr 2003).

The Standard Model of Particle Physics (SMPP) predicts: (i) the Electroweak (EW) phase transition at temperatures of $\sim$ 100 GeV, responsible for the spontaneous breaking of the EW symmetry (e.g. Aoki et al. 2006a) and (ii) the Quantum Chromodynamics (QCD) phase transition at 170 MeV (e.g. Allton et al. 2002; Bernard et al. 2005; Aoki et al. 2006b) related to the spontaneous breaking of the chiral symmetry of the QCD when quarks and gluons become confined in hadrons. At very high temperatures ($T > 172.5$ GeV) all the particles of the SMPP contribute to the effective number of degrees of freedom giving g(T)=106.75 (e.g. Yao et al. 2006; Sobrinho 2011). As the expansion of the Universe goes on, the temperature decreases and, by the temperature of the QCD transition, with the Universe consisting on a Quark-Gluon Plasma (QGP), we have $g_{QGP} = 61.75$. At the end of the QCD transition, when the Universe becomes an Hadronic Gas (HG), we reach $g_{HG} = 17.25$ (e.g. Beringer et al. 2012).

The aim of this paper is to study the behaviour of δ_c during the QCD phase transition. The paper is organized as follows: after reviewing, in Section 2, some key aspects concerning the early Universe and the QCD phase transition we derive, in Section 3, new results for δ_c considering three different models: the Bag Model (BM), the Lattice Fit Model (LFM), and the Crossover Model (CM). In Section 4 we conclude with a general discussion.

We have considered, for the radiation-dominated phase of the Universe, the lowest accepted value of $\delta_c = 0.43$, which corresponds to the Mexican-Hat perturbation profile, a very representative one. Table 1 (Section 2) sums up key observational and derived parameters that we used throughout this paper.

2 THE EARLY UNIVERSE

2.1 The scale factor

We appear to live in a flat, homogeneous and isotropic expanding Universe (at scales > 100 Mpc) well described by the Friedmann-Lemaître-Robertson-Walker (FLRW) metric where the *scale factor*, $a(t)$, describes the time dependence of the Universe geometry: $a(t) \propto t^{1/2}$ for radiation domination, $a(t) \propto t^{2/3}$ for matter domination, and $a(t) \propto \exp(\sqrt{\frac{\Lambda}{3}}ct)$ for dark energy domination, where $\Lambda = 3H_0\Omega_\Lambda c^{-2}$ is the cosmological constant (e.g. Beringer et al. 2012) — see Table 1. A common normalization of the FLRW metric defines the scale factor equal to unity at the present time ($a(t_0) = 1$; e.g. Liddle & Lyth 1993), yielding, for a Universe dominated by a positive cosmological constant (cf. Table 1)

$$a_\Lambda(t) = \exp\left(c\sqrt{\frac{\Lambda}{3}}(t - t_0)\right), \quad t_\Lambda \leqslant t \leqslant t_0 \,. \tag{5}$$

For the matter-dominated Universe we have

$$a_m(t) = a_\Lambda(t_\Lambda)\left(\frac{t}{t_\Lambda}\right)^{2/3}, \ t_{eq} \leqslant t \leqslant t_\Lambda \,. \tag{6}$$

Between the end of inflation at $t = t_e \sim 10^{-33}$ s; (e.g. Narlikar & Padmanabhan 1991) and $t = t_{eq} = 2.37 \times 10^{12}$ s the Universe was radiation-dominated since at the latter instant a radiation-matter equality is reached (Table 1). Exceptions to radiation-domination in the $t_e \leqslant t \leqslant t_{eq}$ time interval might have taken place during cosmological phase transitions such as the QCD (when the Universe might have been dust-like). We, then, split the radiation-domination epoch into three parts. For the interval between the end of the QCD phase transition (t_+) and t_{eq} we define

$$a_{rl}(t) = a_m(t_{eq})\left(\frac{t}{t_{eq}}\right)^{1/2}, \ t_+ \leqslant t \leqslant t_{eq} \,. \tag{7}$$

During the QCD phase transition we define

$$a_{QCD}(t) = a_{rl}(t_+)\left(\frac{t}{t_+}\right)^{n_{qcd}}, \ t_- \leqslant t \leqslant t_+ \tag{8}$$

where $n_{qcd} = 2/3$ if the Universe experiences a QCD dust-like phase or $n_{qcd} = 1/2$ if the Universe continues to be radiation-dominated during that epoch. Finally, between the end of inflation (t_e) and the beginning of the QCD phase transition (t_-) we define

$$a_{rm}(t) = a_{QCD}(t_-)\left(\frac{t}{t_-}\right)^{1/2}, \ t_e \leqslant t \leqslant t_- \,. \tag{9}$$

2.2 Primordial density fluctuations

The simplest way to describe a classical fluctuation with amplitude δ is in terms of an overdensity or density contrast (e.g. Musco, Miller, & Rezzolla 2005)

$$\rho = \overline{\rho}(1 + \delta) \tag{10}$$

where $\overline{\rho}$ represents the average cosmological density. In the unperturbed region we assume the FLRW metric and obtain (Carr 1975)

$$\left(\frac{da}{dt}\right)^2 = \frac{8\pi G}{3}\overline{\rho}(t)a(t)^2 \tag{11}$$

while for the perturbed one we get (Carr 1975)

$$\left(\frac{ds}{d\tau}\right)^2 = \frac{8\pi G}{3}\rho(\tau)s(\tau)^2 - \Delta\epsilon \tag{12}$$

where $\Delta\epsilon$ represents the corresponding curvature constant, τ is the proper time as measured by comoving observers and $s(\tau)$ plays the role of a scale factor for the perturbed region. Considering that, initially, the overdense region is comoving with the unperturbed background, we consider $\tau_k = t_k$, $s_k = a_k$ and $(ds/d\tau)_k = (da/dt)_k$ yielding, for $\Delta\epsilon$, the expression (Carr 1975)

$$\Delta\epsilon = \frac{8\pi G}{3}a_k^2\left(\rho_k - \overline{\rho}_k\right). \tag{13}$$

Inserting this into equation (12) and using equation (10) we obtain

$$\left(\frac{ds}{d\tau}\right)^2 = \frac{8\pi G}{3}\left(\rho(\tau)s(\tau)^2 - \rho_k a_k^2\frac{\delta_k}{1 + \delta_k}\right) \tag{14}$$

Table 1. Observational and derived (the last three) parameters used in our calculations: **(1)** nomenclature; **(2)** description (HG — Hadronic Gas; QGP — Quark-Gluon Plasma); **(3)** numerical value (BM — Bag Model; LFM — Lattice Fit Model); **(4)** reference, if any: [1] Ade et al. (2014); [2] Bennett et al. (2013); [3] Allton et al. (2002); Bernard et al. (2005); Aoki et al. (2006b) [4] Beringer et al. (2012).

(1)	(2)	(3)	(4)
t_0	Age of the Universe	4.36×10^{17} s	[1]
T_0	Cosmic Microwave Background Temperature	2.72548 K	[2]
H_0	Present day value of the Hubble Parameter $H(t)$	67.3 $\mathrm{kms^{-1}Mpc^{-1}}$	[1]
Ω_Λ	Dark energy density parameter	0.685	[1]
t_Λ	Age of the Universe at matter-Λ equality (when the expansion starts to accelerate); equals $2/(3H_0)$	3.06×10^{17} s	—
z_{eq}	Redshift at matter-radiation equality	3391	[1]
t_{eq}	Age of the Universe at matter-radiation equality (from equation (6), considering that $a_m(t_{eq}) = (1 + z_{eq})^{-1}$)	2.37×10^{12} s	—
T_c	The temperature of the Universe at the QCD phase transition	170 MeV	[3]
g_{QGP}	Degrees of freedom for the QGP Universe	61.75	[4]
g_{HG}	Degrees of freedom for the HG Universe	17.25	[4]
t_+	Age of the Universe at the end of the QCD phase transition	1.2×10^{-4} s (BM, LFM)	Section 3
t_-	Age of the Universe at the begining of the QCD phase transition	6.2×10^{-5} s (BM)	Section 3
		9.5×10^{-5} s (LFM)	Section 3

which describes the evolution of the perturbed region.

During the radiation-dominated epoch the Universe can be regarded as a diluted gas with its Equation of State (EoS) written as $p = w\rho$ (e.g. Carr 2003; Ryden 2003) where p is pressure, ρ is cosmological density, and the dimensionless quantity w (the *EoS parameter*) is equal to $\frac{1}{3}$ (e.g. Carr 2003), since the sound speed is $c_s^2 = \left(\frac{\partial p}{\partial \rho}\right)_S = w = \frac{1}{3}$ (e.g. Schmid, Schwarz, & Widerin 1999). If during the QCD phase transition the Universe becomes matter-dominated (pressureless gas), then we get $w = 0$ and $c_s^2 = 0$. Considering that $\rho(t) \propto a(t)^{-3(1+w)}$ (e.g. Beringer et al. 2012) we write $\rho(\tau) = K_s s(\tau)^{-3(1+w)}$ where K_s is a constant and $s(\tau)$ represents the evolution of the scale factor for the perturbed region. Similarly, $\rho_k = K_k a_k^{-3(1+w_k)}$ with w_k the EoS parameter when the fluctuation crosses the horizon. Hence, equation (14) becomes

$$\left(\frac{ds}{d\tau}\right)^2 = \frac{8\pi G}{3}\frac{K_s}{1+\delta_k}\left(\frac{1+\delta_k}{s(\tau)^{1+3w}} - \frac{K_k}{K_s}\frac{\delta_k}{a_k^{1+3w_k}}\right). \quad (15)$$

The turnaround point (t_c) is reached when the perturbed region stops expanding, i.e., when $ds/d\tau = 0$. Thus, evaluating equation (15) at t_c we get

$$s_c^{1+3w_c} = \frac{K_s}{K_k} a_k^{1+3w_k}\left(\frac{1+\delta_k}{\delta_k}\right) \quad (16)$$

which relates the size of the perturbed region at the horizon crossing time with the respective size at the turnaround point. The calculation of the relation K_s/K_k is detailed in Appendix A.

Following Jedamzik & Niemeyer (1999), the value of δ_c during a first order phase transition is only a function of the horizon crossing time t_k and the strength of the transition. We here interpret the latter as the time interval that the fluctuation spends on the mixed phase until the turnaround point (t_c) is reached. We are thus assuming, for our convenience, that when the turnaround point is reached a PBH will form, even if not immediately after the instant t_c (as long as $\delta_k \geqslant \delta_c$). Hence, we are not taking into account the dynamics between the turnaround point and the instant when the PHB actually arises with the formation of an event horizon, which would require to numerically solve the Hernandez-Misner equations for a variable sound speed.

2.3 The QCD phase transition according to three concurrent models

A first order QCD phase transition is characterized by the formation of hadronic bubbles during a short period of supercooling when they grow slowly and the released latent heat maintains the temperature constant until the transition is complete (e.g. Schmid, Schwarz, & Widerin 1999). We consider three concurrent approaches (models) to describe the QCD phase transition which we now describe in detail.

2.3.1 The Bag Model (BM)

The Bag Model (BM) provides a first semiphenomenological description of an EoS that features a quark-hadron first-order transition (e.g. Boyanovsky, de Vega, & Schwarz 2006). The simplest version of the model considers the thermodynamics in two different regions: a high temperature region ($T > T_c$, $t < t_-$) where we have a QGP and a low temperature region ($T < T_c$, $t > t_+$) where we have an HG. In both situations the sound speed is $c_s^2 = 1/3$. At the critical temperature $T = T_c$, i.e. during the time interval $[t_-, t_+]$, quarks, gluons, and hadrons coexist in equilibrium at constant pressure and temperature and the sound speed vanishes (e.g. Boyanovsky, de Vega, & Schwarz 2006).

2.3.2 The Lattice Fit Model (LFM)

In the limit, it is expected that simulations on larger and larger lattices, while making the lattice spacing smaller and smaller, closely match the continuum theory. Here we consider a Lattice Fit Model (LFM) describing a first-order phase transition which was obtained for quenched lattice QCD (gluons only, no quarks), giving similar results to

the case of two-flavour QCD (Schmid, Schwarz, & Widerin 1999). However, now the high-temperature behaviour ($T \sim 4T_c \sim 700$ Mev) is not well described by the Stephan-Boltzmann law, which suggests that even at these high temperatures the plasma is not described by free quarks and gluons (e.g. Boyanovsky, de Vega, & Schwarz 2006). Within the LFM the sound speed is given by (Schmid, Schwarz, & Widerin 1999)

$$c_s^2(T) = \frac{1}{3}\left(1 - \frac{T_c}{T}\right)^{1-\gamma}, \quad T \geqslant T_c \tag{17}$$

with a good fit obtained for $0.3 < \gamma < 0.4$ (in this paper, we thus consider $\gamma = 1/3$). Right after the end of the transition ($T < T_c$) an HG appears (similarly to the BM case) and the sound speed is, once again, $c_s^2 = 1/3$ (Schmid, Schwarz, & Widerin 1999).

2.3.3 The scale factor and the average energy density of the Universe under the BM and the LFM

The evolution of the scale factor during the QGP and HG mixed phase in a first-order QCD transition, i.e., when $c_s^2 = 0$, is determined by the entropy conservation (e.g. Schwarz 2003; Schmid, Schwarz, & Widerin 1997)

$$f_R = \frac{a_{rl}(t_+)}{a_{QCD}(t_-)} = \left(1 + R_l\left(\frac{g_{QGP}}{g_{HG}} - 1\right)\right)^{1/3} \tag{18}$$

with $R_l = 1$ (BM) or $R_l = 0.2$ (LFM).

The evolution of the average energy density $\overline{\rho}$ as a function of time during a first-order QCD transition is given by (Jedamzik 1997)

$$\overline{\rho}(t) = \left(\frac{a_{QCD}(t_-)}{a(t)}\right)^3 (\rho_{QGP}(T_c) + \frac{1}{3}\rho_{HG}(T_c)\Big) - \frac{1}{3}\rho_{HG}(T_c). \tag{19}$$

Taking into account that $\rho_{HG}(T) = \frac{\pi^2}{30} g_{HG} T^4$ and $\rho_{QGP}(T) = \frac{\pi^2}{30} g_{QGP} T^4 + B$, with $B = \frac{\pi^2}{90}(g_{QGP} - g_{HG})\, T_c^4$ (cf. Schmid, Schwarz, & Widerin 1999) equation (19) becomes

$$\overline{\rho}(t) = \frac{1}{3}\frac{\pi^2}{30} T_c^4 \left[4 g_{QGP}\left(\frac{a_{QCD}(t_-)}{a(t)}\right)^3 - g_{HG}\right]. \tag{20}$$

Let ρ_1 and ρ_2 ($\rho_2 = \rho(t_+) < \rho_1 = \rho(t_-)$) be the energy densities at the start and at the end of the QCD phase transition, respectively. For simplicity, we assume for $\rho > \rho_1$ a pure QGP ($w = 1/3$), for $\rho < \rho_2$ a pure HG ($w = 1/3$) and for $\rho_2 < \rho < \rho_1$ a mixed phase, that can be treated as dust ($w = 0$). In order to characterize the horizon crossing time, t_k, and the turnaround point, t_c, in terms of energy density we introduce the quantities x and y defined as $x = \overline{\rho}_k/\rho_1$ ($\overline{\rho}_k$ represents the average cosmological density when $t = t_k$) and $y = \rho_1/\rho_2$. Taking into acount that $\rho_1 = \rho(t_-) = \rho_{QGP}(T_c)$ we have, from equation (20)

$$x(t) = \frac{\overline{\rho}(t_k)}{\rho_1} = \frac{4 g_{QGP}\left(\frac{a_{QCD}(t_-)}{a(t)}\right)^3 - g_{HG}}{4 g_{QGP} - g_{HG}} \tag{21}$$

where $a(t)$ is given by: (i) equation (7) if $x \leqslant y^{-1}$; (ii) equation (8) if $y^{-1} < x < 1$; (iii) equation (9) if $x \geqslant 1$.

2.3.4 The Crossover Model (CM)

An alternative to a first-order phase transition is a simple crossover in thermodynamic behaviour without discontinuities or singularities in the free energy or any of its derivatives. If the crossover is smooth the system will evolve in local thermodynamic equilibrium. This is the situation if during the QCD phase transition only light quarks are present. Now, the sound speed decreases but does not vanish completely (e.g. Boyanovsky, de Vega, & Schwarz 2006). The entropy density for the QCD Crossover Model (CM) can be written as (e.g. Schwarz 1998)

$$S(T) = \frac{2\pi^2}{45} g_{HG} T^3 \left[1 + \frac{1}{2}\left(\frac{g_{QGP}}{g_{HG}} - 1\right) \times \left(1 + \tanh\left(\frac{T - T_c}{\Delta T}\right)\right)\right] \tag{22}$$

where the value of ΔT must be chosen in order to fit the modeled results: the best range of values found for the QCD is $0 \leqslant \Delta T < 0.1 T_c$ (e.g. Schmid, Schwarz, & Widerin 1999; Bernard et al. 1997). When $\Delta T \longrightarrow 0$ we recover the BM (Boyanovsky, de Vega, & Schwarz 2006). We thus chose for the CM the values $\Delta T = 0.1 T_c$ and $T_c = 170$ MeV.

3 THE VALUE OF δ_C DURING THE QCD PHASE TRANSITION

The relation between $a(t)$ and T (the temperature of the Universe evaluated at the same instant) can be written as $a(t) = T_0/T$; in particular, when $t = t_+$ we have $a_{rl}(t_+) = T_0/T_c$ (Table 1) which, together with equation (8), gives

$$t_+ = \frac{t_{eq}}{a_m(t_{eq})^2}\left(\frac{T_0}{T_c}\right)^2. \tag{23}$$

From equations (18) and (8) we get the relation

$$t_- = \frac{t_+}{\sqrt{{f_R}^3}}. \tag{24}$$

Using $T_c = 170$ MeV (Table 1) we obtain, from equation (23), the value $t_+ \approx 1.2 \times 10^{-4}$ s which is valid for both the BM and the LFM. From equation (24) we get $t_- \approx 6.2 \times 10^{-5}$ s (BM) or $t_- \approx 9.5 \times 10^{-5}$ s (LFM). The value of y^{-1}, which defines the end of the transition, can now be determined evaluating $x(t_+)$. It turns out that for the BM case, with $g_{QGP} = 61.75$ and $g_{HG} = 17.25$, we get $y^{-1} \approx 0.225$ and, for the LFM, $y^{-1} \approx 0.632$.

Fluctuation dynamics in the presence of a phase transition are dependent on the strength of the transition, as well as on the exact time t_k at which the fluctuation crosses the horizon: shortly before onset, during, or shortly after completion of the transition (Jedamzik & Niemeyer 1999). For each situation we must also consider the possible locations of the turnaround point t_c when the kinetic energy of expansion is zero and the region begins to collapse. Similarly to what was done by Cardall & Fuller (1998) we consider, in the case of a QCD first-order phase transition, six different classes of density fluctuations (designated A, B, C, D, E, and F). In each case the value of δ_c (cf. equation 4) should de replaced by $\delta_c(1 - f)$ where the function f denotes the fraction of the overdense region spent in the dust-like phase of the transition (Appendix B and Table B1).

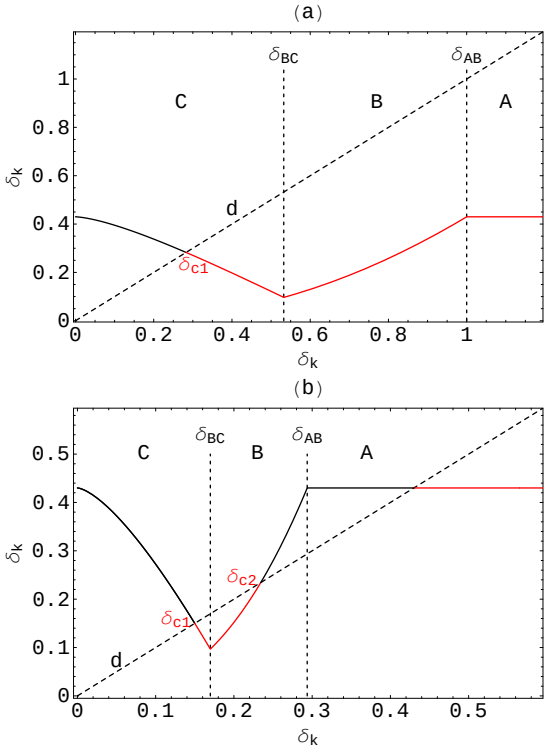

Figure 1. The threshold for PBH formation during the QCD Bag Model (BM) when $\delta_c = 0.43$ and: **(a)** $x = 2$ ($t_k \approx 4.0 \times 10^{-5}$ s); **(b)** $x = 15$ ($t_k \approx 1.1 \times 10^{-5}$ s). The vertical dashed lines labeled "δ_{AB}" and "δ_{BC}" represent the frontiers between the different classes of fluctuations (A, B, and C), which cover the full range of δ_k. The solid curve corresponds to the function $(1-f)\delta_c$ and the dashed curve, labeled "d", to the identity δ_k. A PBH will form if $(1-f)\delta_c < \delta_k$. In (a) this happens when $\delta_k > \delta_{c1} \approx 0.28$ (red curve). In (b) this happens when $\delta_k \in [\delta_{c1} \approx 0.15, \delta_{c2} \approx 0.23]$ and when $\delta_k \geqslant 0.43$ (red curves). See text for more details.

3.1 The Bag Model (BM)

When $x > 1$ ($t_k < t_-$) we are dealing with fluctuations of classes A, B or C (Appendix B and Table B1). For a given x we can determine the range of amplitudes which correspond to each class. For example, when $x = 2$ ($t_k \approx 4.0 \times 10^{-5}$ s) the overdensity will be of class C if $0 < \delta_k < 0.53$, of class B if $0.53 < \delta_k < 1$ and of class A if $\delta_k > 1$. In order to identify the values of δ_k for which collapse to a PBH occurs, when $x = 2$ and $\delta_c = 0.43$, we plot in Figure 1a both $(1-f)\delta_c$ and δ_k itself as functions of δ_k. It turns out that fluctuations of class C with $\delta_k < \delta_{c1} \approx 0.28$ dissipate before forming a PBH: δ_{c1} represents a lower threshold for PBH formation during the QCD phase transition.

As a second example we show in Figure 1b the case $x = 15$ ($t_k \approx 1.1 \times 10^{-5}$ s). There are now two regions for which PBH formation is allowed: (i) a region for $\delta_k \geqslant 0.43$, which corresponds to PBH formation from fluctuations of class A; (ii) a region between $\delta_{c1} \approx 0.15$ and $\delta_{c2} \approx 0.23$ corresponding to the formation of PBHs from fluctuations of classes B and C. The gap between $\delta_k = 0.23$ and $\delta_k = 0.43$ corresponds to: (i) fluctuations of class A which dissipate because they have $\delta_k < 0.43$; (ii) fluctuations of class B which dissipate because they do not spend enough time in the dust-like phase, allowing collapse to begin.

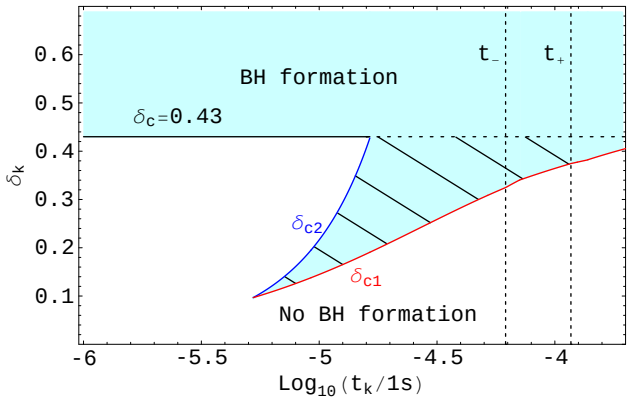

Figure 2. The curve in the $(\log_{10}(t_k/1\mathrm{s}), \delta_k)$ plane indicating which parameter values lead to collapse to a PBH under the QCD Bag Model (BM) when $\delta_c = 0.43$. The vertical lines correspond to the beginning ($t_k = t_-$) and end ($t_k = t_+$) of the QCD phase transition. For a given horizon crossing time, t_k, the dashed region represents the newly found window for PBH formation (cf. Figure 1). The lowest value attained by δ_c occurs at the intersection point $\delta_{c1} = \delta_{c2} = 0.097$. It corresponds to a fluctuation crossing the horizon when $t_k = 5.2 \times 10^{-6}$ s.

In Figure 2 we show the results obtained for the entire QCD Bag Model (BM) when $\delta_c = 0.43$. The intersection point $\delta_{c1} = \delta_{c2} = 0.097$ represents the lowest value attained by δ_c. It corresponds to a fluctuation that lies rigth on the boundary between fluctuations of classes B and C and crosses the horizon at the instant $t_k = 5.2 \times 10^{-6}$ s (cf. Figure B1). Depending on the instant of time that a particular fluctuation crosses the horizon we may have PBH forming from fluctuations of classes B, C, E and F, with the threshold $\delta_c < 0.43$.

3.2 The Crossover Model (CM)

We now assume that the minimum value of the sound speed is reached at $t \approx t_+$ (corresponding to $T \approx T_c$) and that during the QCD the Universe continues to be radiation-dominated ($w = 1/3$) with the scale factor given by equation (8) with $n_{qcd} = 1/2$. Considering that $a(T) = T_0/T$, we obtain

$$T(t) = T_0 \left[a_m(t_{eq}) \left(\frac{t}{t_{eq}} \right)^{1/2} \right]^{-1} . \tag{25}$$

Since the sound speed for a fluid with entropy density S can be written as (e.g. Schmid, Schwarz, & Widerin 1999)

$$c_s^2 = \left(\frac{d \ln S}{d \ln T} \right)^{-1} \tag{26}$$

we get, from equation (22)

$$c_s^2(T) = \left[3 + \frac{T(g_{QGP} - g_{HG})}{\Delta T} \times \right.$$
$$\left. \times \frac{\mathrm{sech}\left(\frac{T-T_c}{\Delta T}\right)^2}{g_{HG} + g_{QGP} + (g_{QGP} - g_{HG})\tanh\left(\frac{T-T_c}{\Delta T}\right)} \right]^{-1} . \tag{27}$$

We now define *effective duration* as the time interval $[t_1, t_2]$ for which the sound speed stays below the 'background' value $c_{s,0}^2 = 1/3$. With the help of equations (25)

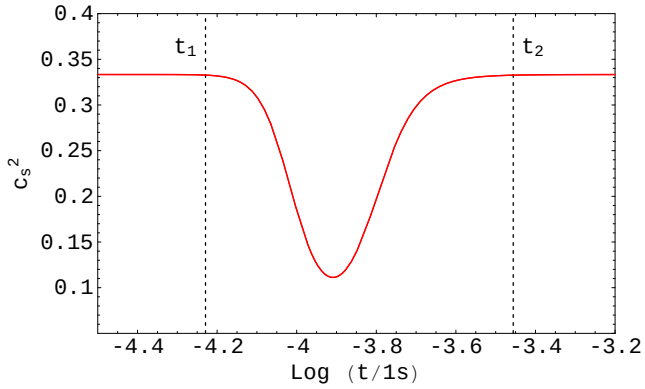

Figure 3. The sound speed $c_s^2(t)$ for the QCD Crossover Model (CM) with a reference temperature $T_c = 170$ MeV and $\Delta T = 0.1T_c$. Between the instants $t_1 \approx 5.9 \times 10^{-5}$ s and $t_2 \approx 3.5 \times 10^{-4}$ s the sound speed stays below its 'background' value $c_{s,0}^2 = 1/3$, reaching a minimum of $c_{s,min}^2 \approx 0.11$ at $t = t_+ = 1.2 \times 10^{-4}$ s.

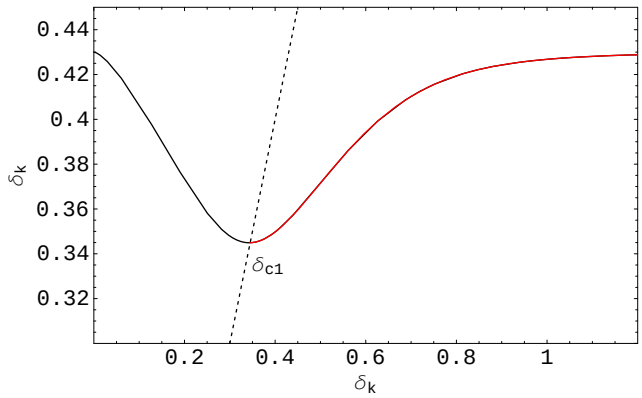

Figure 4. PBH formation during the QCD transition according to the Crossover Model (CM) for the case $\delta_c = 0.43$ and $t_k = 4.2 \times 10^{-5}$ s. The solid curve corresponds to the function $(1-f)\delta_c$ (cf. equation 35) and the dashed curve corresponds to the identity δ_k. The intersection between the two produces our newly found threshold for PBH formation ($\delta_{c1} \approx 0.345$). In red, we show where PBHs can form ($\delta_k > \delta_{c1}$). See the text for more details.

and (27) and by taking $\Delta T = 0.1T_c$ we get $t_1 \approx 5.9 \times 10^{-5}$ s and $t_2 \approx 3.5 \times 10^{-4}$ s. In Figure 3, we show the curve $c_s^2(t)$ with minimum $c_{s,min}^2 \approx 0.11$. Now, taking $w_k = w_c = 1/3$, equation (16) can be written as

$$s_c = a_k \left(\frac{1+\delta_k}{\delta_k} \right)^{1/2}, \tag{28}$$

which is valid for the entire transition. Expressions for s_c and a_k are obtained from the scale factor $a(t)$. Thus, we have

$$a_k = a_m(t_{eq}) \left(\frac{t_k}{t_{eq}} \right)^{1/2} \tag{29}$$

and

$$s_c = a_m(t_{eq}) \left(\frac{t_c}{t_{eq}} \right)^{1/2}. \tag{30}$$

Inserting equations (29) and (30) into equation (28) we obtain a relation between the horizon crossing time t_k and the turnaround time t_c

$$t_c = t_k \frac{1+\delta_k}{\delta_k}. \tag{31}$$

We need to determine the analogous of function f (Table B1) for the CM. This function should account for the fact that we now have a variable sound speed and that a smaller value of $c_s(t)$ contributes more significantly to the reduction of δ_c than a larger one. We then introduce the time function α_{sp} such that

$$\alpha_{sp}(t) = 1 - \frac{c_s(t)}{c_{s0}} \tag{32}$$

where $c_{s0} = 1/\sqrt{3}$. In the case of the BM we have $\alpha_{sp}(t) = 1$ during the mixed phase and $\alpha_{sp}(t) = 0$ otherwise. Now, we consider for the function f a more general equation

$$f = \frac{1}{s_c^3} \int_{s_i}^{s_c} \alpha_{sp}(t) ds^3, \tag{33}$$

where s_i corresponds to the size of the region when the transition begins. Since $s = s(t)$ gives the evolution of the scale factor during the CM we get

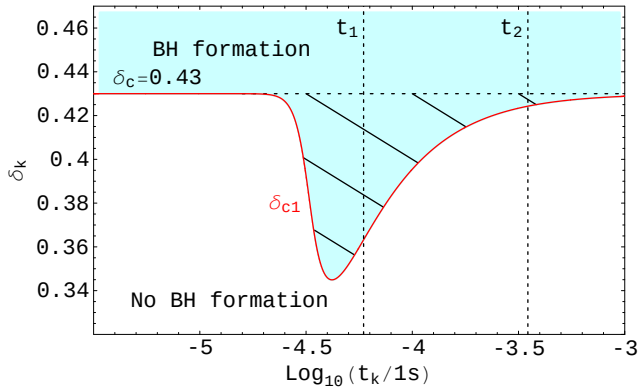

Figure 5. The curve in the $(\log_{10}(t_k/1\mathrm{s}), \delta_k)$ plane indicating which parameter values lead to collapse to a PBH for the QCD Crossover Model (CM) when $\delta_c = 0.43$. The vertical lines $t_1 \approx 5.9 \times 10^{-5}$ s and $t_2 \approx 3.5 \times 10^{-4}$ s define the transition epoch. For a given horizon crossing time, t_k, the dashed region represents our newly found window for PBH formation.

$$ds^3 = \frac{3}{2} a_m(t_{eq})^3 \frac{\sqrt{t}}{t_{eq}^{3/2}} dt. \tag{34}$$

Combining equations (31), (32), (33) and (34) we get

$$f = \frac{3}{2} \left(t_k \frac{1+\delta_k}{\delta_k} \right)^{-3/2} \int_{t_1}^{t_k \frac{1+\delta_k}{\delta_k}} \left(1 - \frac{c_s(t)}{c_{s0}} \right) \sqrt{t} dt. \tag{35}$$

We can now study the changes in the value of the threshold δ_c during the CM following the same method that we used for the BM. In Figure 4 we show, as an example, the case $t_k = 4.2 \times 10^{-5}$ s giving $\delta_{c1} \approx 0.345$ (this is the case in which δ_{c1} reaches the smallest value). Figure 5 shows the region on the $(\log_{10}(t_k/1\mathrm{s}), \delta_k)$ plane for which collapse to a PBH occurs in the case of the CM for $\delta_c = 0.43$.

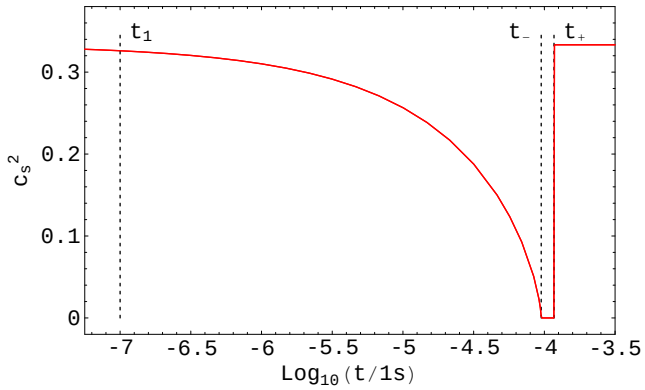

Figure 6. The sound speed $c_s^2(t)$ for the QCD phase transition according to the Lattice Fit Model (LFM) with $T_c = 170$ MeV (Table 1). During the mixed phase, which occurs between $t_- = 9.5 \times 10^{-5}$ s and $t_+ = 1.2 \times 10^{-4}$ s, the sound speed is zero. For $t_1 \approx 10^{-7}$ s the sound speed equals 99% of its 'background' value of $1/\sqrt{3}$.

3.3 The Lattice Fit Model (LFM)

For the evolution of a fluctuation within the QCD Lattice Fit Model (LFM) we adopt a model similar to the one considered for the BM (cf. Appendix B, Table B1, Figure B1, Section 3.1). One difference is that, in the case of the LFM, the mixed phase interval ($t_- < t < t_+$), during which the sound speed vanishes, is shorter. Another difference is that before the mixed phase (i.e. during the last instants of the QGP phase) there is a time interval $t_1 \leqslant t \leqslant t_-$ during which the sound speed drops from $1/\sqrt{3}$ to zero. The sound speed as a function of time for $t \leqslant t_-$ can be written as (cf. equation 17)

$$c_s^2(t) = \frac{1}{3}\left(1 - \frac{a_{rm}(t)}{a_{QCD}(t_-)}\right)^{2/3} = \frac{1}{3}\left[1 - \left(\frac{t}{t_-}\right)^{1/2}\right]^{2/3} \quad (36)$$

We now define $t_1 > t_-$ as the instant for which c_s^2 equals 99% of its 'background' value of $c_{s,0}^2 = 1/3$. From equation (36), with $t_- = 9.5 \times 10^{-5}$ s we get $t_1 \approx 10^{-7}$ s (see Figure 6).

We need to find a function f suitable to the LFM. For the period $t_1 \leqslant t \leqslant t_-$ we proceed as in the CM (cf. Section 3.2) while for the period $t_- \leqslant t \leqslant t_+$ we consider the BM results (cf. Section 3.1). Let us start with fluctuations of class A (see Table B1). We have $f_A = 0$, as in the BM case, only if $t_c < t_1$. In general, for a fluctuation of class A we write (cf. equation 33)

$$f_{A_{LFM}} = \frac{1}{s_{c,A}^3}\int_{s_k}^{s_{c,A}} \alpha_{sp}(t) ds^3 \quad (37)$$

where $s_{c,A}$ is the size of the overdense region at turnaround (cf. Table B1) and $s_k = a_{rm}(t_k)$ the size of the overdense region when the fluctuation crosses the horizon, given by equation (9). Here $\alpha_{sp}(t)$ is given by equation (32), as in the CM, but now with the sound speed $c_s(t)$ given by equation (36). Since the volume element $ds^3 = 3s^2 ds = 3s^2 \frac{ds}{dt} dt$ must be evaluated in the radiation-dominated epoch ($t_k \leqslant t \leqslant t_-$), we have, from equation (9), that

$$ds^3 = \frac{3}{2} a_{QCD}(t_-)^3 \frac{\sqrt{t}}{(t_-)^{3/2}} dt. \quad (38)$$

Inserting equation (38) into equation (37) and using $a_{rm}(t_k)$ from equation (9) in $s_{c,A}$ (Table B1), we obtain

$$f_{A_{LFM}} = \frac{3}{2}\left(t_k \frac{1+\delta_k}{\delta_k}\right)^{-3/2} \int_{t_k}^{t_k \frac{1+\delta_k}{\delta_k}} \alpha_{sp}(t)\sqrt{t} dt. \quad (39)$$

In the case of fluctuations of classes B and C (Table B1) we write, respectively

$$f_B = f_{B_{LFM}} + \frac{s_{c,B}^3 - s_1^3}{s_{c,B}^3} = \\ = \frac{1}{s_{c,B}^3}\int_{s_k}^{s_1} \alpha_{sp}(t) ds^3 + \frac{s_{c,B}^3 - s_1^3}{s_{c,B}^3} \quad (40)$$

$$f_C = f_{C_{LFM}} + \frac{(s_2)_C^3 - s_1^3}{s_{c,C}^3} = \\ = \frac{1}{s_{c,C}^3}\int_{s_k}^{s_1} \alpha_{sp}(t) ds^3 + \frac{(s_2)_C^3 - s_1^3}{s_{c,C}^3} \quad (41)$$

where s_1 and $(s_2)_C$ represent the size of the overdense region when, respectively, $t = t_-$ and $t = t_+$ (cf. equations A4 and A6) and $s_{c,B}$ and $s_{c,C}$ is the size of the overdense region at turnaround for, respectively, classes B and C (cf. Table B1). Inserting equation (38) into equations (40) and (41), using $a_{rm}(t_k)$ in $s_{c,B}$ and $s_{c,C}$ and considering that $s_1 = a_{QCD}(t_-)$, we get

$$f_{B_{LFM}} = \frac{3}{2}\left(t_k^{-1/2} x_k^{-1/4} \frac{(1+\delta_k)^{3/4}}{\delta_k}\right)^{-3} \\ \times \int_{t_k}^{t_-} \alpha_{sp}(t)\sqrt{t} dt \quad (42)$$

$$f_{C_{LFM}} = \frac{3}{2}\left(t_k \frac{1+\delta_k}{\delta_k}\right)^{-3/2} y^{-1/2} \int_{t_k}^{t_-} \alpha_{sp}(t)\sqrt{t} dt. \quad (43)$$

In the case of fluctuations of classes E and F ($t_k > t_-$) we continue to use, respectively for f_E and f_F, the same expressions that we did in the case of the BM (Table B1).

Following the same method that we used for the BM and the CM we have determined the threshold δ_c for the entire QCD phase transition according to the LFM. As a result, we obtain Figure 7. Within the LFM our newly found window for PBH formation occurs between δ_{c1} and δ_c, and δ_{c1} and δ_{c2}; also, due to the decrease on the sound speed value between the instants t_1 and t_- (cf. Figure 6) we have a new window for PBH formation from fluctuations of class A betwwen δ_{cA} and δ_c. The intersection point $\delta_{c1} = \delta_{c2} = 0.15$ represents the lowest value attained by δ_c. It corresponds to a fluctuation that lies rigth on the boundary between fluctuations of classes B and C and crosses the horizon at the instant $t_k = 1.2 \times 10^{-5}$ s. Depending on the instant of time when a particular fluctuation crosses the horizon we might have PBH forming from fluctuations of classes A, B, C, E, and F, with the threshold $\delta_c < 0.43$.

3.4 Summary of results (the three models compared)

We have determined the evolution ot the PBH formation threshold (δ_c) during the QCD phase transition within three different models: Bag Model (BM), Crossover Model (CM),

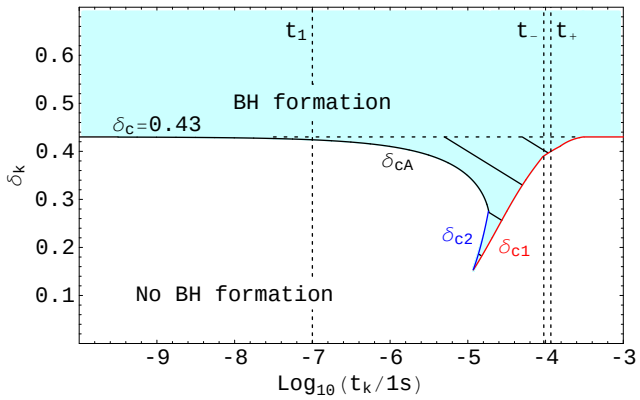

Figure 7. The curve on the $(\log_{10}(t_k/1s),\ \delta_k)$ plane indicating which parameter values lead to collapse to a PBH in the case of the QCD Lattice Fit Model (LFM) when $\delta_c = 0.43$. The vertical lines correspond to $t_k = t_1 \approx 10^{-7}$ s, $t_k = t_- = 9.5 \times 10^{-5}$ s, and $t_k = t_+ = 1.2 \times 10^{-4}$ s (cf. Figure 6). For a given horizon crossing time, t_k, the dashed region represents our newly discovered window for PBH formation. The lowest value attained by δ_c occurs at the intersection point $\delta_{c1} = \delta_{c2} = 0.15$. It corresponds to a fluctuation crossing the horizon when $t_k = 1.2 \times 10^{-5}$ s.

and Lattice Fit Model (LFM). Taking into account that the value of δ_c is related to the particular perturbation profile considered, we chose to work with $\delta_c = 0.43$, corresponding to the Mexican-hat perturbation. This 'background' value of δ_c, which is valid for a radiation-dominated Universe, might decrease during the QCD phase transition, as a result of the reduction of the sound speed, improving the chances of PBH formation.

In the case of the BM, we initially followed the literature (Section 3.1). Since the sound speed vanishes during the interval $[t_-, t_+] \simeq [6.2 \times 10^{-5}, 1.2 \times 10^{-4}]$s, a new window for PBH formation appears (cf. Figure 2) with the threshold for PBH formation reaching its absolute minimum value $(\delta_{c,min})$ at the intersection point $\delta_{c1} = \delta_{c2} = 0.097$.

For the CM (Section 3.2) and the LFM (Section 3.3) we derived our own set of equations based on the behaviour of the sound speed during the QCD transition. Within the CM we found that the sound speed decreases smoothly to a minimum value of $c_s^2 = 0.11$, without vanishing, and rises again to its background value of $c_{s,0}^2 = 1/3$ (Figure 3). Hence, a new window for PBH formation, between δ_{c1} and δ_c, was discovered (cf. Figure 5) with the threshold for PBH formation reaching the minimum value $\delta_{c,min} = 0.345$.

As regards the LFM model, the sound speed also vanishes during the interval $[t_-, t_+] \simeq [9.5 \times 10^{-5}, 1.2 \times 10^{-4}]$s (as in the BM) while it is gradually reduced during the time interval $[t_1, t_-] \simeq [10^{-7}, 9.5 \times 10^{-5}]$s (cf. Figure 6). Hence, we treated the interval $[t_1, t_-]$ as in the CM and, the interval $[t_-, t_+]$ as in the BM (cf. Section 3.3). As a result, we discovered, besides the new windows for PBH formation $[\delta_{c1}, \delta_{c2}]$ and $[\delta_{c1}, \delta_c]$ similar to the ones found on the BM, a hitherto unknown LFM window for PBH formation $[\delta_{cA}, \delta_c]$ (Figure 7), reflecting the contribution from the period $[t_1, t_-]$ (cf. Figure 6). Within the LFM we found $\delta_{c,min} = 0.15$.

In Table 2 we summarize the results obtained for $\delta_{c,min}$ during the QCD phase transition according to the BM (Figure 2), CM (Figure 5), and LFM (Figure 7). In the case of the BM we obtained a reduction of $\Delta\delta_c/\delta_c \approx 77\%$, while for the CM this is about 20% and in the case of the LFM 65%.

Table 2. The minimum value reached by the PBH formation threshold $(\delta_{c,min})$ within the Bag, Crossover, and Lattice Fit Models (Figures 2, 5, and 7, respectively) as well as the corresponding percentual decrease $(\Delta\delta_c/\delta_c)$ with respect to the background value $\delta_c = 0.43$. Also shown, in each case, is the corresponding instant of the horizon crossing time (t_k).

Model	$\delta_{c,min}$	$\Delta\delta_c/\delta_c(\%)$	t_k (s)
Bag (BM)	0.097	77%	5.2×10^{-6}
Crossover (CM)	0.345	20%	4.2×10^{-5}
Lattice Fit (LFM)	0.15	65%	1.2×10^{-5}

4 DISCUSSION

In order for the collapse of an overdense region in the early Universe forming a PBH, we must have $\delta_k > \delta_c$ where δ_k is the amplitude of the density fluctuation perturbation and δ_c a critical value which is related to the particular perturbation profile shape. We chose to work with $\delta_c = 0.43$ since it corresponds to the representative Mexican-hat perturbation profile. Although the value of δ_c remains constant during the radiation-dominated epoch, it can experience important reductions during cosmological phase transitions, which lead to a higher probability $\beta(t_k)$ of forming PBHs.

In particular, at the QCD phase transition $\sim 1\ M_\odot$ PBHs might be formed (Carr et al. 2010), even if only constituting a small fraction of the dark halo objets (e.g. Tisserand et al. 2007), they are not completely ruled out. A population of even smaller PBHs might also have formed, according to the scaling law given by equation (3).

In this paper we explored the behaviour of δ_c during the QCD phase transition under three diferent models: Bag Model (BM), Crossover Model (CM), and Lattice Fit Model (LFM) and obtained reductions of 20% (CM), 65% (LFM), and 77% (BM) – cf. Table 2.

Assuming, for example, $\sigma^2(t_k) = 2.3 \times 10^{-4}$ (cf. Sobrinho 2011) we get, for a radiation-dominated Universe ($\delta_c = 0.43$), $\beta(t_k) \sim 10^{-177}$ (equation 4), a negligible value. Our new results, however, show that δ_c can get as low as 0.097 (BM; Table 2), which implies the much higher probability of $\beta(t_k) \sim 10^{-10}$, which lies very close to the observational constraints at the QCD epoch (cf. Carr et al. 2010). Although the BM is the one that offers the best prospects as regards PBH formation, even in the case of the CM (a much smoother event: compare Figures 2 and 5) an important contribution to PBH formation is still expectable. Assuming, for example, $\sigma^2(t_k) = 2.0 \times 10^{-3}$ we get $\beta(t_k) \sim 10^{-14}$.

Our next step will be to find an appropriate expression for the mass variance at horizon crossing, so that we might estimate the fraction of the Universe going into PBHs during the QCD epoch and, consequently, their cosmological density. This might be very relevant towards understanding the dark matter halo build-up in the Galaxy and in other galaxies.

ACKNOWLEDGEMENTS

The authors are very grateful to Anne Marie Green for useful comments and observations made on this work. They also acknowledge helpful discussions with the referee whose valuable comments improved this paper substantially. All the Figures within this paper were created with the help of Wolfram Research, Inc., Mathematica, Version 5.1, Champaign, IL (2004).

APPENDIX A: CALCULATION OF THE RELATION K_S/K_K

Referring back to equation (16) and to the constants K_s and K_k, for classes A and F (see Appendix B and Table B1), which evolve completely during a radiation-dominated phase, and class D, which evolves completely during the mixed phase, we have $K_s/K_k = 1$. In the case of class B, the change in the value of the EoS parameter (from $w_k = 1/3$ to $w_c = 0$) occurs when $t = t_-$, or equivalently, when $x = 1$ ($x = \overline{\rho}_k/\rho_1$ with $\overline{\rho}_k$ representing the average cosmological density when $t = t_k$ and ρ_1 the energy density at the start of the phase transition; cf. Section 2.3.3). Considering that $\rho(\tau) \propto a(\tau)^{-3(1+w)}$ is a continuous function, we write, $K_k s_1^{-3(1+w_k)} = K_s s_1^{-3(1+w_c)}$, where s_1 represents the size of the overdense region at the beginning of the transition. This leads to

$$\left(\frac{K_s}{K_k}\right)_B = \frac{s_1^{3w_c}}{s_1^{3w_k}} = \frac{1}{s_1}. \tag{A1}$$

In the case of class E the change of the EoS parameter (from $w_k = 0$ to $w_c = 1/3$) occurs when $t = t_+$ or, equivalently, when $x = y^{-1}$ ($y = \rho_1/\rho_2$ with ρ_2 representing the energy density at the end of the phase transition; cf. Section 2.3.3). The continuity of the density ρ now leads to

$$\left(\frac{K_s}{K_k}\right)_E = \frac{s_2^{3w_c}}{s_2^{3w_k}} = (s_2)_E \tag{A2}$$

where s_2 represents the size of the overdense region at the end of the transition.

In the case of fluctuations of class C there is an intermediate period when $w = w' = 0$. Applying the continuity condition for ρ successively at $t = t_+$ and $t = t_-$ we obtain

$$\left(\frac{K_s}{K_k}\right)_C = \frac{s_2^{3w_c}}{s_1^{3w_k}}\frac{s_1^{3w'}}{s_2^{3w'}} = \frac{(s_2)_C}{s_1}. \tag{A3}$$

The expression for s_1 (common to classes B and C) can be obtained considering that ρ_1 is reached from radiation domination (i.e. $\rho_1 \propto s_1^{-4}$ and $\rho_k \propto a_k^{-4}$). From energy conservation we have the condition $\rho_1 s_1^4 = \rho_k a_k^4$ which can be combined with equation (10) in order to obtain

$$s_1 = x^{1/4}(1+\delta_k)^{1/4} a_k. \tag{A4}$$

An expression for $(s_2)_E$ is obtained considering that ρ_2 is reached from the mixed phase (i.e. $\rho_2 \propto s_2^{-3}$ and $\rho_k \propto a_k^{-3}$). From energy conservation we have the condition $\rho_2 s_2^3 = \rho_k a_k^3$ which can be combined with equation (10) in order to obtain

$$(s_2)_E = (xy)^{1/3}(1+\delta_k)^{1/3} a_k. \tag{A5}$$

An expression for $(s_2)_C$ is obtained considering that a fluctuation of class C spans the entire mixed phase. From energy conservation we have the condition $\rho_2 s_1^3 = \rho_k s_2^3$ yielding

$$(s_2)_C = s_1 y^{1/3} \tag{A6}$$

with s_1 given by equation (A4). Finally, in the case of fluctuations of class F, which evolve completely during the radiation-domination phase, we have

$$(s_2)_F = (xy)^{1/4}(1+\delta_k)^{1/4} a_k. \tag{A7}$$

The values here derived in equations (A1-A7) are used to calculate the fraction of the overdense region spent in the dust-like phase of the QCD phase transition (f, in the last column of Table B1).

APPENDIX B: CLASSES OF FLUCTUATIONS

Fluctuation dynamics in the presence of a phase transition are dependent on the strength of the transition, as well as on the horizon crossing time t_k and on the turnaround point t_c where the collapse begins (Jedamzik & Niemeyer 1999). In order to consider all possible solutions, we define six classes of density fluctuations labeled A, B, C, D, E, and F (Table B1). In each case the value of the PBH formation threshold δ_c (cf. equation 4) must de replaced by $\delta_c(1-f)$ where f denotes the fraction of the overdense region spent in the dust-like phase of the transition.

The boundary between two neighbouring classes X and Y can be determined taking into account that it occurs where $\delta_c(1-f_X) = \delta_c(1-f_Y)$. For example, for the separation between classes A and B we get the condition $x(t_k) = (1+\delta_k)/\delta_k^2$ (see Sobrinho 2011, for a detailed discussion).

The boundary between classes C and D turns out to be a single point

$$y = \left(\frac{1+\delta_k}{\delta_k}\right)^3 \approx \frac{1}{0.225} \Rightarrow \delta_k \approx 1.55 \tag{B1}$$

meaning that class D fluctuations do not exist for $\delta_k < 1.55$ and class C ones for $\delta_k > 1.55$. Since, in our study, we are looking for values of δ_c that are always less or equal to 0.43, class D is thus ruled out.

The use of six different classes of fluctuations works as an intermediate step towards determining the evolution of δ_c during the QCD phase transition. In Figure B1 we reproduce Figure 2 but now including very detailed explanations on five fluctuation classes (D is not represented — cf. equation B1). In it, the points f1, f2, f3, and f4, for example, represent fluctuations with increasing amplitude δ that cross the horizon at the same instant $t_k = 2\times10^{-5}$ s before the beginning of the QCD phase transition.

We now use these four example points by following the details in both Figure B1 and Table B1. f1, the point with the largest amplitude (δ) develops faster, reaching the turnaround point (not represented) before t_-. Therefore it is classified as a fluctuation of class A. f2 represents a fluctuation of class B: although it crosses the horizon before t_-, the turnaround point is reached only during the mixed phase because now we have a fluctuation with a smaller amplitude which develops slower. f3 represents a fluctuation of class C: it starts before t_- and ends after t_+, crossing the all phase

Table B1. Classification of overdense regions according to the state of matter at the horizon crossing time (t_k) and at the turnaround point (t_c) for the QCD phase transition. We are using a convention first proposed by Cardall & Fuller (1998). **(1)**: fluctuation class (class D fluctuations are shown only for the sake of completeness, since they are ruled out in our study — we are looking for values of δ_c that are always less or equal to 0.43 and class D fluctuations do not exist when $\delta_k < 1.55$ (cf. equation B1)); **(2)**: the state of matter at the horizon crossing time (t_k); HG — Hadronic Gas; QGP — Quark-Gluon Plasma; mixed — mixture of HG and QGP; **(3)**: EoS parameter at horizon crossing; $w = 1/3$ — radiation-dominated Universe; $w = 0$ — matter-dominated Universe; **(4)**: the state of matter at the turnaround point (t_c); **(5)**: EoS parameter at turnaround; **(6)**: the scale factor of the overdense region at turnaround (cf. equation 16) — $x = \overline{\rho}_k/\rho_1$ and $y = \rho_1/\rho_2$ ($\overline{\rho}_k$ represents the average cosmological density when $t = t_k$, ρ_1 and ρ_2 are the energy densities at the start and at the end of the phase transition, respectively), a_k is the size of the overdense region when $t = t_k$; **(7)**: the fraction of the overdense region spent in the dust-like phase of the transition – s_1 and s_2 represent the size of the overdense region at the start and at the end of the phase transition, respectively (cf. equations A4–A7).

(1)	**(2)**	**(3)**	**(4)**	**(5)**	**(6)**	**(7)**
Class	t_k	w_k	t_c	w_c	s_c	f
A	QGP	1/3	QGP	1/3	$a_k \left(\frac{1+\delta_k}{\delta_k}\right)^{1/2}$	0
B	QGP	1/3	mixed	0	$a_k \frac{x^{-1/4}(1+\delta_k)^{3/4}}{\delta_k}$	$\frac{s_{c,B}^3 - s_1^3}{s_{c,B}^3}$
C	QGP	1/3	HG	1/3	$a_k y^{1/6} \left(\frac{1+\delta_k}{\delta_k}\right)^{1/2}$	$\frac{(s_2)_C^3 - s_1^3}{s_{c,C}^3}$
D	*mixed*	*0*	*mixed*	*0*	$a_k \frac{1+\delta_k}{\delta_k}$	$\frac{s_{c,D}^3 - s_1^3}{s_{c,D}^3}$
E	mixed	0	HG	1/3	$a_k (xy)^{1/6} \frac{(1+\delta_k)^{2/3}}{\delta_k^{1/2}}$	$\frac{(s_2)_E^3 - s_1^3}{s_{c,E}^3}$
F	HG	1/3	HG	1/3	$a_k \left(\frac{1+\delta_k}{\delta_k}\right)^{1/2}$	$\frac{(s_2)_F^3 - s_1^3}{s_{c,F}^3}$

transition in between. In the case of f1, f2, and f3 we have PBH formation. On the other hand, f4 represents a fluctuation with amplitude below the threshold for PBH formation. It crosses the QCD phase transition and dissipates without reaching a turnaround point.

In the case of an unperturbed region the beginning of the QCD phase transition occurs at t_- and the end at t_+. If the region is perturbed, however, the evolution is slower. For example, when $t_k = 7 \times 10^{-5}$ s, although the average cosmological background is already on the mixed phase ($t_- < t_k < t_+$), an overdense region with, for example, $\delta_k = 0.6$ remains on the QGP phase — e.g. point f5 in Figure B1: such regions do not expand with the rest of the background Universe (the state of matter on those regions evolves slower).

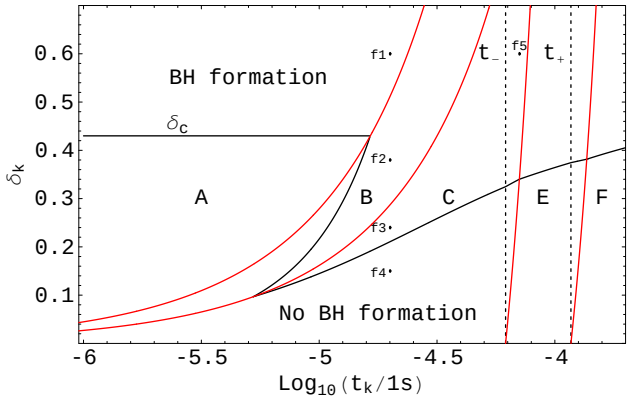

Figure B1. Regions in the plane $(\log_{10}(t_k/1\text{s}), \delta_k)$ corresponding to the classes of fluctuations listed in Table B1 for the BM case: the black line labeled "δ_c" represents the PBH formation threshold during the QCD phase transition according to this model(Section 3.1, Figure 2). The red lines split the plane into slices, each one corresponding to a different class of fluctuations — A, B, C, E, or F (D is not represented because this class only exists for $\delta_k > 1.55$ — cf. equation B1, Table B1). The points f1, f2, f3, and f4 represent fluctuations with different amplitudes δ that cross the horizon at the same instant $t_k = 2 \times 10^{-5}$ s during the QGP phase. The point $f5$ represents a fluctuation which crosses the horizon at the instant $t_k = 7 \times 10^{-5}$ s. These five points are used as an explanatory example in the text.

REFERENCES

Ade P. A. R., et al., 2014, A&A, 571, A16
Allton C. R., Ejiri S., Hands S. J., Kaczmarek O., Karsch F., Laermann E., Schmidt C., Scorzato L., 2002, Phys. Rev. D, 66, 074507
Aoki Y., Endrődi G., Fodor Z., Katz S. D., Szabó K. K., 2006a, Nature, 443, 675
Aoki Y., Fodor Z., Katz S. D., Szabó K. K., 2006b, Phys. Lett. B, 643, 46
Bennett C. L., et al., 2013, ApJS, 208, 20

Beringer J., et al., 2012, Phys. Rev. D, 86, 010001
Bernard S., Rischke D. H., Maruhn J. A., Greiner W., 1997, Nuc. Phys. A, 625, 473
Bernard C., et al., 2005, Phys. Rev. D, 71, 034504
Blais D., Bringmann T., Kiefer C., Polarski D., 2003, Phys. Rev. D, 67, 024024
Boyanovsky D., de Vega H. J., Schwarz D. J., 2006, Annual Review of Nuclear and Particle Science, 56, 441
Bringmann T., Kiefer C., Polarski D., 2002, Phys. Rev. D, 65, 024008
Cardall C. Y., Fuller G. M., 1998, preprint (astro-ph/9801103)
Carr B. J., 1975, ApJ, 201, 1
Carr B. J., 2003, in D. Giulini, C. Kiefer and C. Lämmerzahl, eds, Lecture Notes in Physics, Vol. 631, Quantum Gravity: From Theory to Experimental Search. Springer, Berlin, p. 301
Carr B. J., Hawking S. W., 1974, MNRAS, 168, 399
Carr B. J., Kohri K., Sendouda Y., Yokoyama J., 2010, Phys. Rev. D, 81, 104019
Green A. M., 2015, in Calmet X., ed., Quantum Aspects of Black Holes. Springer, London, p. 129
Harada T., Yoo C.-M., Kohri K., 2013, Phys. Rev. D, 88, 084051
Hawking S., 1971, MNRAS, 152, 75
Jedamzik K., 1997, Phys. Rev. D, 55, 5871
Jedamzik K., Niemeyer J. C., 1999, Phys. Rev. D, 59, 124014
Khlopov M. Y., 2010, Research in Astronomy and Astrophysics, 10, 495
Liddle A. R., Lyth D. H., 1993, Physics Reports, 231, 1
Musco I., Miller J. C., 2013, Class. Quantum Grav., 30, 145009
Musco I., Miller J. C., Polnarev A. G., 2009, Class. Quantum Grav., 26, 235001
Musco I., Miller J. C., Rezzolla L., 2005, Class. Quantum Grav., 22, 1405
Narlikar J. V., Padmanabhan T., 1991, ARA&A, 29, 325
Niemeyer J. C., Jedamzik K., 1999, Phys. Rev. D, 59, 124013
Novikov I. D., Polnarev A. G., Starobinskii A. A., Zeldovich I. B., 1979, A&A, 80, 104
Polarski D., Dolgov A., 2001, Int. J. Mod. Phys. D, 10, 927
Polnarev A. G., Musco I., 2007, Class. Quantum Grav., 24, 1405
Ryden B., 2003, Introduction to Cosmology. Pearson Eduction, Inc., publishing as Addison Wesley, San Francisco.
Schmid C., Schwarz D. J., Widerin P., 1997, Phys. Rev. Lett., 78, 791
Schmid C., Schwarz D. J., Widerin P., 1999, Phys. Rev. D, 59, 043517
Schwarz D. J., 1998, Mod. Phys. Lett. A, 13, 2771
Schwarz D. J., 2003, Annalen der Physik, 515, 220
Sobrinho J. L. G., 2011, PhD thesis, Univ. da Madeira available at: http://digituma.uma.pt/handle/10400.13/235
Sobrinho J. L. G., Augusto P., 2014, MNRAS, 441, 2878
Tisserand P., et al., 2007, A&A, 469, 387
Yao W.-M., et al., 2006, Journal of Physics G, 33, 1